

MOX–Report No. 01/2011

**Dimensional Reduction of Functional Data by means of
Principal Differential Analysis**

M. DALLA ROSA, LAURA M. SANGALLI, SIMONE VANTINI

MOX, Dipartimento di Matematica “F. Brioschi”
Politecnico di Milano, Via Bonardi 9 - 20133 Milano (Italy)

mox@mate.polimi.it

<http://mox.polimi.it>

Dimensional Reduction of Functional Data by means of Principal Differential Analysis

M. Dalla Rosa ^a, L. M. Sangalli ^b, S. Vantini ^b

^a Eni S.p.A. Divisione E&P, San Donato M.se, Italy

^b MOX– Modellistica e Calcolo Scientifico
Dipartimento di Matematica “F. Brioschi”
Politecnico di Milano

Piazza Leonardo da Vinci 32, 20133 Milano, Italy

matilde.dalla.rosa@eni.it

laura.sangalli@polimi.it

simone.vantini@polimi.it

Keywords: Functional data analysis, Dimensional reduction.

AMS Subject Classification: 62H30, 62H25, 62P10.

Abstract

We explore the use of principal differential analysis (PDA) as a tool for performing dimensional reduction of functional data sets. In particular, we compare the results provided by PDA and by functional principal component analysis (FPCA) in the dimensional reduction of three synthetic data sets, and of a real data set concerning 65 vascular geometries (i.e., the AneuRisk data set). The analyses of the synthetic data sets show that PDA can provide an alternative and effective representation of functional data that is always easily interpretable in terms of constant, exponential, sinusoidal, or damped-sinusoidal functions and not affected by the presence of clusters or strong correlations among the original components. Moreover, in the analysis of the AneuRisk data set, PDA is able to detect important features of the data that FPCA is not able to detect.

1 PDA as a Dimensional Reduction Tool

PDA is a technique that enables the estimation of a differential operator from a functional data set. This technique has already been used to analyze various types of applications such as the study of free handwriting ([3]), economic models ([8]), weather ([4]) and chemical models ([2]). In those papers, the main goal of PDA

was the estimation of the the unknown parameters of a well known underlying differential operator. In our case, the operator is instead used as a tool for achieving a better understanding of the phenomenon. In fact, the estimated operator becomes a tool for obtaining a convenient representation of the data. It provides a finite-dimensional space onto which the data can be projected and where the variability related to linear relations among derivatives can be explored.

In order to estimate a linear differential operator L of order m with constant coefficients by means of PDA, the observed functions x_i , $i = 1, \dots, N$ need to be contained in the Sobolev space $H^m(a, b)$. Given this assumption, a natural procedure to estimate the operator L is to choose the estimate \hat{L} such that it minimizes the sum of squared differential residuals

$$RSS(L) = \sum_{i=1}^N \|Lx_i\|_{L^2(a,b)}^2, \quad (1)$$

over all linear differential operators L of the form

$$Lx_i = D^m x_i - \beta_{m-1} D^{m-1} x_i - \dots - \beta_1 D x_i - \beta_0 x_i. \quad (2)$$

The minimization problem (1) is solved for the value $\hat{\beta} = -\mathbf{R}^{-1}\mathbf{s}$ of the parameter vector $\beta = (\beta_0, \beta_1, \dots, \beta_{m-1})'$, with $(\mathbf{R})_{j_1 j_2} = \sum_{i=1}^N \langle D^{j_1} x_i, D^{j_2} x_i \rangle_{L^2(a,b)}$ and $(\mathbf{s})_{j_1} = \sum_{i=1}^N \langle D^{j_1} x_i, D^m x_i \rangle_{L^2(a,b)}$ with $j_1, j_2, \dots \in \{0, 1, \dots, m-1\}$.

The estimation of the linear operator L and the Partitioning Principle of Hilbert spaces (e.g. [5]), jointly enable the orthogonal decomposition of the functional space the data belong to, into two different components $ker(\hat{L})$ and $ker(\hat{L})^\perp$, where $ker(\hat{L})$ is the m -dimensional linear space of all functions \hat{x} satisfying the linear differential relation $\hat{L}\hat{x} = 0$ and $ker(\hat{L})^\perp$ is its orthogonal counter part. This means that for $i = 1, \dots, N$, the function x_i can be univocally decomposed in the sum of two orthogonal components \hat{x}_i and \hat{e}_i (named structural and residual component, respectively) such that $x_i = \hat{x}_i + \hat{e}_i$, $\hat{L}\hat{x}_i = 0$, and $\hat{L}\hat{e}_i = \hat{L}x_i$.

Due to the orthogonality of \hat{x}_i and \hat{e}_i , the structural component \hat{x}_i turns out to be the solution of the following minimization problem:

$$\min_{x \in ker(\hat{L})} \|x - x_i\|_{L^2(a,b)}^2 \quad \text{for } i = 1, \dots, N, \quad (3)$$

that, because of the finite dimensionality of $ker(\hat{L})$, reduces to $\hat{x}_i(s) = \sum_{j=1}^m \hat{c}_{ij} e^{\hat{\lambda}_j s}$, with $\hat{\lambda}_j$ being the m different complex roots of the characteristic polynomial $\lambda^m - \hat{\beta}_{m-1} \lambda^{m-1} - \dots - \hat{\beta}_1 \lambda - \hat{\beta}_0$ and $(\hat{c}_{i1}, \hat{c}_{i2}, \dots, \hat{c}_{im})' = -\bar{\mathbf{R}}^{-1} \bar{\mathbf{s}}_i$, where $(\bar{\mathbf{R}})_{j_1 j_2} = \langle e^{\hat{\lambda}_{j_1} s}, e^{\hat{\lambda}_{j_2} s} \rangle_{L^2(a,b)}$ and $(\bar{\mathbf{s}}_i)_{j_1} = \langle e^{\hat{\lambda}_{j_1} s}, x_i(s) \rangle_{L^2(a,b)}$. Finally, $\hat{e}_i = x_i - \hat{x}_i$.

A useful tool to measure the effectiveness of the obtained dimensional reduction is the quantity RSQ introduced in [4]. Under the assumption of constant coefficients, RSQ is a ratio between the structural variability and the overall variability. Indeed $RSQ = 1$ when there is only structural variability (i.e., $x_i = \hat{x}_i$ for

$i = 1, 2, \dots, N$) and $RSQ = 0$ when there is no structural variability (i.e., $x_i = \hat{e}_i$ for $i = 1, 2, \dots, N$).

A couple of theoretical remarks about the dimensional reduction achieved by means of the projection of functional data onto $\ker(\hat{L})$ need to be mentioned.

The first remark pertains to the link between PDA and functional regression. Note that, while in the minimization problem (3), N actual functional regression analyses are performed (the only unusual feature with respect to a traditional functional regression is that the regressors are not known but estimated in a previous stage of the analysis), in the minimization problem (1), the link is instead just formal and not pertaining to the modeling. Indeed, in (1), the functional “regressors” $D^j x_i$, $j = 0, \dots, m - 1$, are not deterministic and the random functional “error” Lx_i is not independent from the functional “regressors”.

The second remark pertains instead to the link between PDA and functional principal component analysis (FPCA). Differently from FPCA, where the dimensional reduction is driven just by the point-wise values of the functional data along the domain (a, b) , the dimensional reduction obtained by PDA is driven by the values of linear combinations of the first m derivatives along the domain (a, b) . By definition, FPCA is expected to provide an effective dimensional reduction in any situation where most of the functional variability is expressed within a finite dimensional subspace; at the same time a simple analytical expression of the principal components is often missing and the interpretation of these components is often non-trivial. On the contrary, PDA is expected to provide an effective dimensional reduction only in those situations where most of the functional variability is expressed within some particular finite dimensional subspaces, i.e., the ones generated by some functions of the form $e^{(\alpha \pm \omega i)s}$ with α and $\omega \in \mathbb{R}$; despite of its reduced applicability, PDA always provides very clear results that are easily interpretable in terms of constant, exponential, sinusoidal, or damped-sinusoidal functions.

Since the effectiveness of PDA is related to particular finite dimensional subspaces, it is straightforward that the dimensional reduction provided by FPCA is always more effective or at least comparable with the one provided by PDA. It is thus clear that in all situations where FPCA provides an effective dimensional reduction while PDA does not, the use of the latter is not suggested. It is more interesting to determine if PDA can be a useful tool to have a better insight of the functional variability when both PDA and FPCA provide an effective dimensional reduction. To unravel this doubt, in Section 2, we compare the results of PDA and FPCA in the analysis of three very simple synthetic data sets that can be effectively reduced by both techniques (i.e., data sets made of sinusoids of fixed frequency with random amplitude, horizontal and vertical shifts). In particular, we will show that the presence of strong correlations, or of clusters, strongly depletes the interpretability of the principal components making them unable to reveal the simple nature of the phenomenon, while this is not affecting the results of PDA.

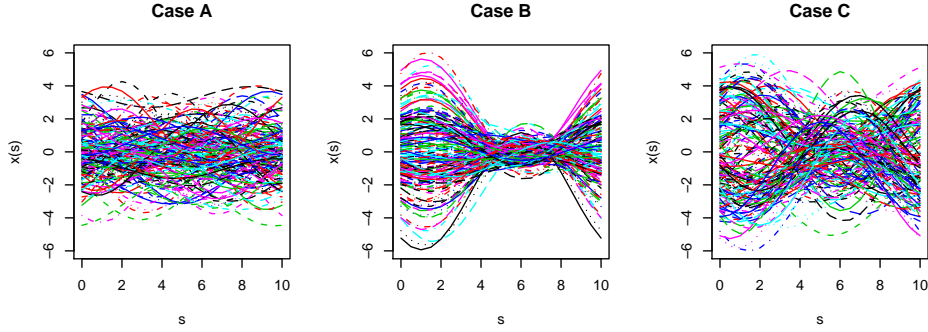


Figure 1: The three synthetic data sets.

2 Comparing FPCA and PDA of three synthetic data sets

In this section we perform the dimensional reduction of three synthetic data sets (Figure 1), made of $N = 200$ functions generated according the model $y_i(s) = a_i + b_i \sin\left(\frac{2\pi}{10}s\right) + c_i \cos\left(\frac{2\pi}{10}s\right)$, with $s \in [0, 10]$, $i = 1, \dots, 200$, and the random coefficients $(a_i \ b_i \ c_i)' \sim iid \mathcal{N}_3(\mu, \Sigma)$:

Case A: $\mu = \mathbf{0}$ and $\Sigma = \mathbf{I}$;

Case B: $\mu = \mathbf{0}$ and $\Sigma = \begin{pmatrix} 1 & 0.9 & 0.9 \\ 0.9 & 1 & 0.9 \\ 0.9 & 0.9 & 1 \end{pmatrix}$;

Case C: $\mu = \mathbf{1}$ for $i = 1, \dots, 100$, $\mu = -\mathbf{1}$ for $i = 101, \dots, 200$, and $\Sigma = \mathbf{I}$.

Note that $\{1, \sin\left(\frac{2\pi}{10}s\right), \cos\left(\frac{2\pi}{10}s\right)\}$ is an orthogonal basis for the three-dimensional space which all functions belong to, and that this space coincides with $\ker(D^3 + \left(\frac{2\pi}{10}\right)^2 D)$. It is thus obvious that both the projection on the first three sample principal components and the projection on the kernel of a third-order operator estimated as in (1), are expected to be effective dimensional reduction tools, and indeed they are. In Figure 2 the basis proposed by FPCA is compared with the basis detected by PDA in the three cases.

In case A, the non-correlation of the original components makes the basis detected by FPCA almost identical to the basis detected by PDA with the first component nearly constant and the remaining two components associated to periodic oscillations.

In case B, due to the strong correlation among original components, the basis detected by FPCA drifts away from the basis detected by PDA, which instead remains unchanged. The constant and sinusoidal terms are indeed confounded in a unique component explaining more than 90% of the total variability. If the model behind the data had not been known, and FPCA had been used to perform dimensional reduction, probably just the first principal component would have been taken

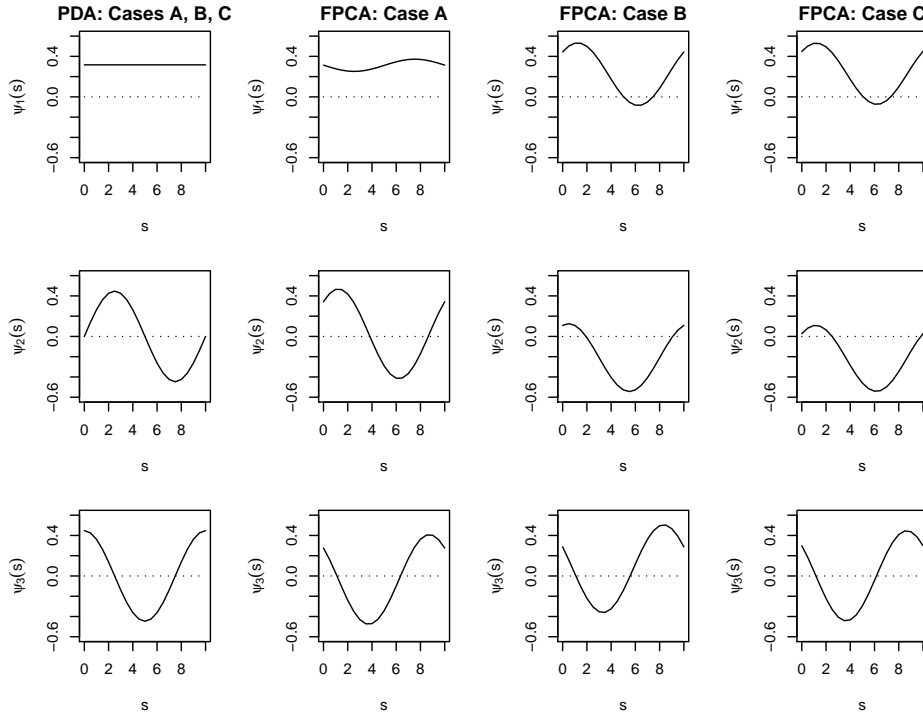


Figure 2: First column: basis functions ψ_1 , ψ_2 , ψ_3 detected by PDA in case A, B, and C (results are graphically undistinguishable). Second, third, and fourth columns: basis functions (principal components) detected by FPCA in case A, B, and C respectively.

into account and interpreted as describing the amplitude variability within a semi-period heuristically identified, and the simple description of functions as a sum of a constant term and a sinusoidal term would have probably remained unrevealed.

In case C, a strong correlation among original components is artificially induced by the presence of two well separated clusters of data. As expected, the first principal component detects the direction connecting the two clusters. This direction is not associated to just one of the original components and thus, similarly to the former case, along this principal component all three original components are put together masking once again the simple description of functions as a sum of a constant term and a sinusoidal term.

Note that PDA provides explicit estimates of the frequency of the sinusoidal component while in FPCA the latter can be estimated just heuristically by comparing subsequent maxima. This is not a big issue in this ideal case where no error component is added, but it could become an issue in favor of PDA in real applications where a 100% effective dimensional reduction is hardly achievable. On the other hand, differently from FPCA, PDA necessitates the estimate of the first m derivatives of each function and not just of the function itself. Once again this is

not an issue in these synthetic cases where derivatives are known exactly, but in real applications an efficient estimation of derivatives could be tough (as shown in [6]).

On the whole, these easy examples show how PDA, when able to effectively reduce functional data dimensionality, can be able to provide an alternative and easily interpretable representation of functional data in terms of constant, exponential, sinusoidal, or damped-sinusoidal functions.

3 FPCA of Internal Carotid Artery Radius

In this section we briefly sketch out the study of the radius of the inner carotid artery performed by means of FPCA in [7], to enable the comparison with the new PDA-based analysis.

The aim of both analyses is to test a conjecture grounded on practical experience at Neuroradiology Department of the Niguarda Ca'Granda Hospital in Milan where data have been collected (E. Boccardi, personal communication): “cerebral arteries of patients with an aneurysm [i.e., malformations of cerebral vessels characterized by a bulge of the vessel wall] at or after the terminal bifurcation of the internal carotid artery [ICA] show peculiar geometric features”.

The AneuRisk¹ data set is based on three-dimensional angiographies of 65 patients. According to the location of the aneurysm and to the conjecture above, the 65 patients can be divided into two groups: Lower group (thirty-two patients that are healthy or affected by aneurysm before the terminal bifurcation of the ICA) and Upper group (thirty-three patients that are affected by aneurysm at the ICA terminal bifurcation or after it).

The raw data set consists of 65 sets of measures of the ICA radius (one set for each patient). For each patient, the ICA radius is sampled along a very dense discrete grid, differing from patient to patient, that is indexed by means of an approximated curvilinear abscissa associated to the vessel centerline ([1]). Such data are clearly functional in nature, although they are sampled in a discrete way. An accurate functional representation of the radii and of their derivatives, is obtained by means of free-knot regression splines of order five. This method provides in fact accurate estimates of derivatives, as it is shown in [6], where free-knot splines are generalized to the case of multidimensional curves. Moreover, in order to enable meaningful comparisons across patients, the 65 ICA radius functions are then registered by means of the alignment procedure described in [7].

In [7] the first two principal components (explaining the 66% and 13% of the total variance, respectively) turn out to be amenable of a biological interpretation. The first one is interpretable as an average size of the carotid (distinguishing be-

¹The AneuRisk project involves MOX (Dip. di Matematica, Politecnico di Milano), LaBS (Dip. di Ingegneria Strutturale, Politecnico di Milano), Istituto Mario Negri (Ranica), Ospedale Niguarda Ca' Granda (Milano), and Ospedale Maggiore Policlinico (Milano), and is supported by Fondazione Politecnico di Milano and Siemens Medical Solutions Italia.

tween narrow and wide ICAs), while the second one as a tapering factor (distinguishing between cylindrical and conic ICAs).

From the analysis of the associated scores, it appears that the patients belonging to the Upper group present more tapered and wider carotids, with a lower within-group variability in the size of the radius than the Lower group.

4 PDA of Internal Carotid Artery Radius

In this section we present the PDA of the 65 internal carotid artery radius functions introduced in Section 3. As already stated, the focus is on the possible relations between the patient's ICA radius and his membership to the Lower or Upper group.

The first two problems that need to be jointly solved are (i) finding the order m of the linear operator \hat{L} , reaching a compromise between a satisfactory goodness of fit and an easy interpretability of the results, and (ii) finding out if one operator alone (i.e., \hat{L}^{Tot}) is able to explain the variability within the two groups or if two different operators are needed (i.e., \hat{L}^{Low} and \hat{L}^{Up}).

In the following table, the *RSQ* achieved by performing a PDA with $m = 2$ and $m = 3$ for the Lower, the Upper, and the two groups together are reported:

<i>RSQ</i>	\hat{L}^{Low}	\hat{L}^{Up}	\hat{L}^{Tot}
$m = 2$	< 1%	< 1%	< 1%
$m = 3$	36%	29%	33%

It is evident from the previous table that linear differential operators of order two are not able to explain any significant portion of the functional variability of any of the two groups. On the other hand, linear differential operators of order three are able to explain nearly one third of the overall variability in both groups. This means that nearly one third of the functional variability lies within a three-dimensional space, i.e., the kernel of the corresponding operator. We choose $m = 3$ to be the suitable order of the linear differential operator and we decide not to move to a higher order to avoid the use of possibly inaccurate estimates of high order derivatives.

Focusing on third order operators, the minor difference between the *RSQ* associated to \hat{L}^{Low} and \hat{L}^{Up} leaves space for the possibility that \hat{L}^{Tot} can jointly explain the structural variability of both groups. Since no inferential tool is available to test this hypothesis, we heuristically proceed by comparing the roots of two characteristic polynomials of \hat{L}^{Low} and \hat{L}^{Up} . The similarity of the three roots supports our final choice of using $\ker(\hat{L}^{Tot})$ as the three-dimensional space onto which to project all 65 ICA radius functions.

Let us now characterize $\ker(\hat{L}^{Tot})$. Using the procedure presented in Section 1 the third order operator is estimated as follows:

$$\hat{L}^{Tot}x = D^3x + 0.0217D^2x + 0.2940D^1x + 0.0021x, \quad (4)$$

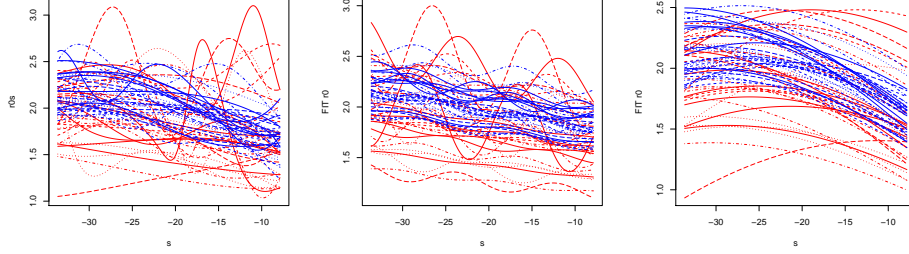


Figure 3: The original radius functions R_i (left), their projections onto $\ker(\hat{L}^{Tot})$ for $m = 3$ (center) and $m = 2$ (right). Blue lines indicate Upper group patients while red ones Lower group patients.

with $\hat{\lambda}_1 = -0.0072$, $\hat{\lambda}_2 = -0.0072 + 0.5400i$, and $\hat{\lambda}_3 = -0.0072 - 0.5400i$ being the three roots of the associated characteristic polynomial, and $\{\hat{\psi}_1, \hat{\psi}_2, \hat{\psi}_3\}$ being a practical real-valued basis associated to them:

$$\hat{\psi}_1(s) = e^{-0.0072s}, \quad \hat{\psi}_2(s) = e^{-0.0072s} \cos(0.5400s), \quad \hat{\psi}_3(s) = e^{-0.0072s} \sin(0.5400s).$$

Due to the very small values of the real parts of the three roots, the first basis function $\hat{\psi}_1$ defines a slightly decreasing function and the remaining basis functions $\hat{\psi}_2$ and $\hat{\psi}_3$ jointly define a nearly sinusoidal function of period 11.6 mm with arbitrary phase.

In the left plot of Figure 3, the 65 ICA radius functions R_i are reported (red color for the Lower group and blue color for the Upper one). The central plot of Figure 3 shows instead the 65 structural components \hat{R}_i of the previous functions, computed as shown in Section 1. For comparison, in the right plot of the same figure, the result achieved using a second order operator is reported.

Most of the 65 ICA radius functions R_i (left plot of Figure 3) present a very similar behavior with the exception of five curves presenting very “unusual” oscillations. It is surprising to what extent the third order operator \hat{L}^{Tot} is able to jointly describe both the 60 “usual” and the five “unusual” ICA radius functions. In [7], the dimensional reduction achieved by FPCA completely smooths those unusual oscillations, letting them be explained by high order principal components. This discrepancy points out the fact that, even if the values of these five ICA radius functions are unusual, the linear relations among the derivatives are not unusual but similar to the ones presented by the other 60 functions.

The last part of the analysis is within a more traditional functional data analysis framework; indeed we now want to analyze the structural variability pointed out by PDA. In particular, we want to perform a FPCA restricted to $\ker(\hat{L}^{Tot})$, in order to identify within this three-dimensional space a new origin and a new set of basis functions that are statistically optimal (i.e., with zero-mean and uncorrelated sample components).

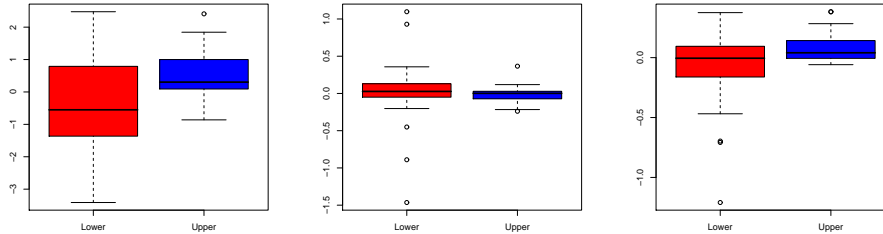


Figure 4: Boxplots of the scores the first, second, and third principal components within $\ker(\hat{L}^{Tot})$ for $m = 3$ (left, center, right respectively) for the Upper and the Lower groups.

The structural variability is strongly dominated by its first functional principal component. Indeed, the first, the second, and the third principal components of the structural variability account for 92%, 5%, and 3% of the structural total variance, respectively.

The first component is strongly associated with ψ_1 and accounts for the average amplitude of the radius along the ICA, thus being a scale factor among patients; the latter two are essentially rotations of ψ_2 and ψ_3 and thus jointly describe sinusoidal oscillations of period 11.6 mm. In Figure 4, the boxplots of the scores for the Upper and the Lower groups corresponding to the first, second, and third principal components within $\ker(\hat{L}^{Tot})$ are reported. It is evident from these scores that the first component discriminates between the two groups in terms of both location and dispersion. Upper group patients seem to have wider carotids than Lower group patients and a lower within-group variability. Moreover some outliers appear along the second and third principal components.

In order to statistically quantify such differences between the two groups we perform three Wilcoxon tests for comparing the median values of the scores of the two groups. The corresponding p -values are 0.7%, 11.0%, and 2.0% for the first, the second, and the third principal component, respectively, pointing out a significant difference in the median values of the first principal component scores for the two groups.

Moreover, not surprisingly, for the Lower group the scores associated to the second and third principal components appear to be very far from the normal distribution (p -values of the Shapiro-Wilk test both much less than 0.1%), supporting the idea that these two principal components are accounting for the structural variability of the “unusual” radius functions. On the other hand, there is no evidence of the absence of normality for the scores associated to the first principal component, neither for the Lower group nor for the Upper group (p -values of the Shapiro-Wilk test 45.3% and 41.9% respectively).

Assuming the normality of the scores associated to the first principal component, we thus perform an F-test for testing the equality of the variances of the

groups. The associated p -value is much less than 0.1%, strongly supporting the hypothesis of two different variances for the two groups.

Reading the results of the previous tests in the light of the interpretations of the functional principal components within $\ker(\hat{L}^{Tot})$ we can draw some interesting conclusions.

Nearly one third of the functional variability of the 65 ICA radius functions of the AneuRisk data set can be described by the third order linear differential equation $\hat{L}^{Tot}x = 0$ with \hat{L}^{Tot} as reported in (4). This variability is essentially due to a term defining the average radius of each ICA and a second one defining the amplitude and the phase of sinusoidal oscillations of the radius with period 11.6 mm.

Most of the structural variability (93%) is associated to the former component (the average radius of each ICA). Along this component the Lower group and the Upper group present different behaviors in terms of both location and dispersion: in particular the Upper group patients (the ones that are affected by aneurysm at the ICA terminal bifurcation or after it) present wider ICA than the Lower group patients (the ones that are healthy or affected by aneurysm before the terminal bifurcation of the ICA). Moreover, the variance of the average radius of the Upper group results significantly lower than the one of the Lower group, making the former group a very well defined group in terms of average radius.

Some patients, all belonging to the Lower group, present some anomalously large oscillations of the ICA radius, that should be further investigated from a medical point of view. On the other hand, except for these few cases, oscillations of the radius represent a minor mode of variability and no significant differences appear evident between the two groups from this perspective.

The conclusions about the average radius of the ICA are in complete agreement with the results drawn in [7]. Conclusions about the oscillations of the ICA radius are instead specific of the present analysis, indeed nothing similar is pointed out by the FPCA performed in [7]. This is not surprising since these oscillations, even if large, do not occur for similar values of the abscissa, and thus FPCA - that, differently from PDA, focuses just on punctual values of the functions - is not able to recognize them as a unique variability feature. On the other hand, contrary to [7], the present analysis does not point out anything regarding the tapering of the terminal part of the ICA.

5 Conclusions

The conclusions drawn in the application to the AneuRisk data set together with the analysis of the synthetic data sets show that PDA can be a useful tool, alternative to FPCA, for performing a dimensional reduction of a functional data set. In particular, when effective as a dimensional reduction tool, PDA (i) can provide a representation of functional data more easily interpretable than FPCA, (ii) this representation is not affected, differently by FPCA, by the presence of clusters or

strong correlations among the original components, and *(iii)* it can detect important features of the data that FPCA is not able to detect.

References

- [1] Antiga L., Piccinelli M., Botti L., Ene-Iordache B., Remuzzi A., Steinman D.A. (2008): An image-based modeling framework for patient-specific computational hemodynamics, *Medical and Biological Engineering and Computing*, **46**, 1097-1120.
- [2] Poyton A.A., Varziri M.S., McAuley K.B., McLellan P-J., Ramsay J.O. (2006): Parameter estimation in continuous-time dynamic models using principal differential analysis. *Computer and chemical engineering* **30**, 698-708.
- [3] Ramsay J.O. (2000): Functional components of variation in handwriting. *Journal of the American Statistical Association* **95**, 9-16.
- [4] Ramsay J.O., Silverman B.W. (2005): *Functional data analysis II* Ed.. Springer-Verlag, NY.
- [5] Rudin W. (1991): *Functional analysis, II* Ed.. McGraw-Hill, NY.
- [6] Sangalli L.M., Secchi P., Vantini S., Veneziani A. (2009): Efficient estimation of three-dimensional curves and their derivatives by free-knot regression splines, applied to the analysis of inner carotid artery centerlines. *Journal of the Royal Statistical Society*, vol **58**, Part 3, 285–306.
- [7] Sangalli L.M., Vantini S., Secchi P., Veneziani A. (2009): A Case Study in Exploratory Functional Data Analysis: Geometrical Features of the Internal Carotid Artery. *Journal of the American Statistical Association*, Vol. **104**, n. 485, 37–48.
- [8] Wang S., Jank W., Shmueli G., Smith P. (2008): Modeling price dynamics in eBay auctions using differential equations. *Journal of the American Statistical Association*, Vol. **103**, n. 483, 1100–1118.

MOX Technical Reports, last issues

Dipartimento di Matematica “F. Brioschi”,
Politecnico di Milano, Via Bonardi 9 - 20133 Milano (Italy)

- 01/2011** M. DALLA ROSA, LAURA M. SANGALLI, SIMONE VANTINI:
*Dimensional Reduction of Functional Data by means of
Principal Differential Analysis*
- 43/2010** GIANCARLO PENNATI, GABRIELE DUBINI,
FRANCESCO MIGLIAVACCA, CHIARA CORSINI,
LUCA FORMAGGIA, ALFIO QUARTERONI,
ALESSANDRO VENEZIANI:
*Multiscale Modelling with Application to
Paediatric Cardiac Surgery*
- 42/2010** STEFANO BARALDO, FRANCESCA IEVA,
ANNA MARIA PAGANONI, VALERIA VITELLI:
*Generalized functional linear models for recurrent events:
an application to re-admission processes in heart failure patients*
- 41/2010** DAVIDE AMBROSI, GIANNI ARIOLI, FABIO NOBILE,
ALFIO QUARTERONI:
*Electromechanical coupling in cardiac dynamics:
the active strain approach*
- 40/2010** CARLO D’ANGELO, ANNA SCOTTI:
*A Mixed Finite Element Method for Darcy Flow in Fractured Porous
Media with non-matching Grids*
- 39/2010** CARLO D’ANGELO:
*Finite Element Approximation of Elliptic Problems with Dirac Measure
Terms in Weighted Spaces. Applications to 1D-3D Coupled Problems*
- 38/2010** NANCY FLOURNOY, CATERINA MAY, PIERCESARE SECCHI:
*Response-adaptive designs in clinical trials for targeting the best
treatment: an overview*
- 37/2010** MARCO DISCACCIATI, ALFIO QUARTERONI,
SAMUEL QUINODOZ:
Numerical approximation of internal discontinuity interface problems
- 36/2010** GIANNI ARIOLI, HANS KOCH:
*Non-Symmetric low-index solutions for a symmetric boundary value
problem*

35/2010 GIANNI ARIOLI, HANS KOCH:
Integration of dissipative PDEs: a case study